

## STRESS ANALYSIS ON SPLIT RING

Y. B. Deshmukh<sup>1</sup>, Dr. D. V. Bhope<sup>2</sup>

<sup>1</sup>M-Tech (CAD/CAM) Student IV semester,  
Rajiv Gandhi College of Engineering Research & Technology, Chandrapur-442401

<sup>2</sup>Professor "Mechanical Engineering Department"  
Rajiv Gandhi College of Engineering Research & Technology, Chandrapur-442401

\*\*\*

**Abstract** - In the present work, the finite element approach is used to evaluate the stresses in the rotating split ring and split ring subjected to bending moment with central circular by varying the diameter and size of hole present at various pitch circle diameter on split ring. An effort is made to study the effect of 4 numbers of holes and 8 numbers of holes on stress concentration factor in the split ring. This analysis reveals that the stress distribution & its magnitude in the split ring are affected due to split angle, size and number of discontinuities.

**Key Words:** Split Ring, Rotating, Bending.

### NOTATION

$R_i$  inner diameter (mm)  
 $R_o$  outer diameter (mm)  
 $D_1$  Outer diameter of ring (mm)  
 $D_2$  Inner diameter of ring (mm)  
 $E$  Modulus of Elasticity (N/mm<sup>2</sup>)  
 $\nu$  Poisson ratio  
 $\rho$  Density of material (Kg/mm<sup>3</sup>)  
 $\omega$  Angular velocity of ring (red/sec)  
 $N$  Rotation of ring  
 $\theta$  Angles (Degree)  
 $\sigma_\theta$  Hoop stress & tangential stress (MPa)  
 $\sigma_r$  Radial stress (MPa)  
 $d$  Diameter of hole (mm)  
 $D_p$  Pitch circle diameter (mm)  
 $d$  Diameter of hole (mm)  
 SCF stress concentration factor

### 1. INTRODUCTION

Split ring or retaining ring is used for locating machine part. These elements are snapped into a circumferential groove machined in a shaft or a housing to form an artificial shoulder.

They are installed into a groove creating a shoulder that retains the assembly. Retaining rings are more efficient and cost-effective than traditional fasteners like screws, nuts, bolts, cotter pins, washers and more, and they do it with a minimum amount of surface preparation to either shaft or housing<sup>(1,2)</sup>. They are subjected to centrifugal loads in case of rotation and also the bending loads.

The finite element approach is used to evaluate the stresses in the rotating split ring with central hole by varying the diameter of hole present at various pitch circle diameters  $D_p$  on split ring.

Later, the finite element approach is used to evaluate the stresses in the split ring with central hole subjected to bending moment with central hole by varying the diameter of hole present at various pitch circle diameters  $D_p$  on split ring. The bending load is applied by considering the pressure of  $P = 100 \text{ N/mm}^2$  acting normal to the split faces.

The various geometric parameter ratios considered for present analysis are as follows,

$D_1 = 200 \text{ mm}$ ,  $D_2 = 100 \text{ mm}$   
 $\theta = 10^\circ, 45^\circ, 90^\circ, 135^\circ \& 180^\circ$   
 $d = 10, 20, 30, \text{ and } 40 \text{ mm}$   
 $D_p/D = 0.5, 0.6, 0.7, 0.8, 0.9, \text{ and } 1.0$

The geometry of split ring without hole and with holes is shown in fig. 1.1 & 1.2 respectively.

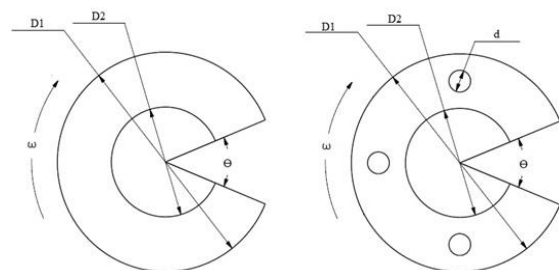


Fig. 1.1 Solid Split Ring

Fig. 1.2 Split Ring with Hole

The ring has a modulus of elasticity ( $E$ )  $200 \times 10^3 \text{ MPa}$  ( $\text{N/mm}^2$ ) and Poisson's ratio ( $\nu$ ) 0.3 which is rotating at 1000rpm, and material density ( $\rho$ ) of  $7.8 \times 10^{-6} \text{ kg/mm}^3$ .

For each and every combination of the above set of geometric parameter values the stress magnitude in the ring are obtained for the load case of the split ring rotating at speed " $\omega$ " and subjected to bending moment load " $P$ ".

## 2. ANALYTICAL & FE ANALYSIS OF FULL RING

There are mainly two types of stresses induced in the rotating ring i.e., radial stress and hoop stress as given by following equations.

The equation for a solid ring is as follows,

Radial stress,  $\sigma_r = \frac{3+v}{8} \rho \omega^2 (R_o - R_i)^2$  with Maximum value of stress is at  $\sqrt{R_i R_o}$

Hoop stress,  $\sigma_\theta = \frac{\rho \omega^2}{4} [(1 - \nu)R_i^2 + (3 + \nu)R_o^2]$  with Maximum value of stress is at inner radius  $R_i$

The hoop stress and radial stress can be evaluated using analytical equation as follows,

Hoop stress can be calculated as follows,

Hoop stress,  $\sigma_\theta$  Max at  $r = a$

$$\text{Hoop stress, } \sigma_\theta = \frac{\rho \omega^2}{4} [(1 - \nu)R_i^2 + (3 + \nu)R_o^2]$$

$$\frac{7.8 \times 10^{-6} * (104.67)^2}{4} [(1 - 0.3) * 50^2 + (3 + 0.3)50^2]$$

$$\sigma_\theta = 742.393 \text{ MPa (N/mm}^2\text{)}$$

Radial stress can be calculated as follows,

Radial stress,  $\sigma_r$  Max at  $r = \sqrt{R_i R_o}$

$$\text{Radial stress, } \sigma_r = \frac{3+v}{8} \rho \omega^2 (R_o - R_i)^2$$

$$= \frac{3+0.3}{8} * 7.8 \times 10^{-6} * (104.67)^2 * (100 - 50)^2$$

$$\sigma_r = 88.125 \text{ MPa (N/mm}^2\text{)}$$

FE approach is also used to determine stress in the full ring and the comparison between the FE Result and analytical results is given in Table 2.1.

**Table 2.1** Comparison of FE and Analytical Results

Stresses	FE (MPa)	Analytical (MPa)
$\sigma_\theta$	92.152	88.125
$\sigma_r$	747.537	742.393

It is observed from Table 2.1 that the analytical stresses and FE stresses are in close agreement. This justifies the validity of FE approach.

## 3. STRESS ANALYSIS OF ROTATING SOLID SPLIT RING

The finite element approach is used to evaluate the stresses in the rotating split ring with central hole by varying the split angles as 10°, 45°, 90°, 135°, and 180°. The body force is applied corresponding to angular velocity  $\omega = 104.67$  rad/sec about Z-axis. The figure 3.1 and 3.2 shows the Von-mises stress contour for various split angles. The FE results are given in Table 3.1.

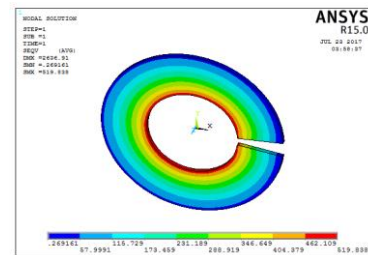


**Fig. 3.1:** Von-mises contour for split angle of 10°

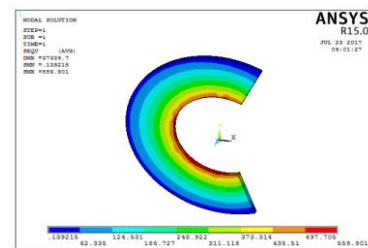


**Fig. 3.2:** Von-mises Stress Contour for split angle 135°

**Table 3.1:** stress comparison of rotating full split ring

Split angle "θ"	1st Principle stress N/mm <sup>2</sup>	2nd Principle stress N/mm <sup>2</sup>	Von-mises stress N/mm <sup>2</sup>	Stress w. r. t. split ring SCF=σ/σ <sub>0</sub>
FULL	380.68	139.972	337.494	-
10°	516.394	24.35	519.838	1.039676
45°	506.811	24.438	519.135	1.03827
90°	681.169	57.112	629.481	1.258962
135°	566.189	85.385	559.901	1.119802
180°	532.665	24.119	535.997	1.071994

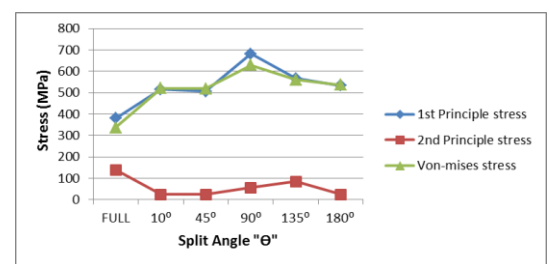


**Fig. 3.1:** Variation of Stresses with Respect to Split Angle

In fig.3.1, 1<sup>st</sup> principle and Von-mises stresses in split ring increases till the split angle of 90° and it remains almost constant after split angle of 90°. It is also observed that radial stresses are lesser in magnitude as compared to hoop stresses.

## 4. STRESS ANALYSIS OF ROTATING SPILT RING WITH HOLES

In the present work, the finite element approach is used to evaluate the stresses in the rotating split ring with central hole by varying the diameter of hole present at various pitch circle diameters on split ring. An effort is made to study the

effect of 4-number of holes and 8-number of holes on stress concentration factor in the split ring.

The stresses are determined in rotating split ring by varying the split angle as 10°, 45°, 90°, 135°, & 180°. In this study, the following cases are considered to evaluate the stresses in rotating split ring with 4-holes and 8-holes which are situated at pitch circle diameter  $D_p$  corresponding to the various ratio of  $D_p/D$ .

- Case 1 Split ring with holes, for  $D_p/D = 0.75$
- Case 2 split ring with holes, for  $D_p/D = 0.5$
- Case 3 Split ring with holes, for  $D_p/D = 0.6$
- Case 4 Split ring with holes, for  $D_p/D = 0.7$
- Case 5 Split ring with holes, for  $D_p/D = 0.8$
- Case 6 Split ring with holes, for  $D_p/D = 0.9$
- Case 7 Split ring with holes, for  $D_p/D = 1.0$

Variation of SCF for  $D_p/D=0.75$  are shown in fig. 4.1 and 4.2

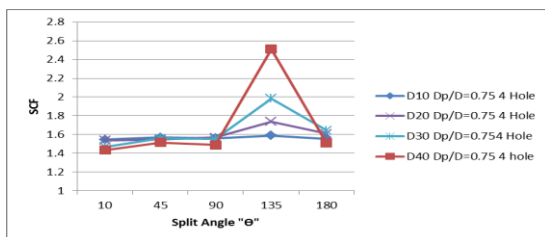


Fig.4.1: Variation of SCF for  $D_p/D = 0.75$  (4-holes)

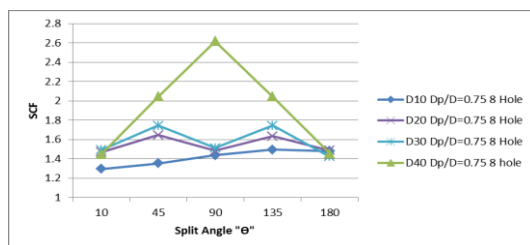


Fig.4.2: Variation of SCF for  $D_p/D = 0.75$  (8-holes)

Fig. 4.1 indicates that the stress concentration factor (SCF) in rotating split ring remain almost constant up to 90° then it suddenly increases till split angle of 135° and decreases till 180°. It observed that the maximum SCF is for the split angle of 135°.

In fig. 4.2, it is observed that the hole diameter of 40 mm leads to maximum stress concentration factor in the split ring. It is seen that the hole diameter of 10 mm leads to increase in the SCF with respect to split angle variation.

Variation of SCF for  $D_p/D=0.5$  are shown in fig. 4.3 and 4.4

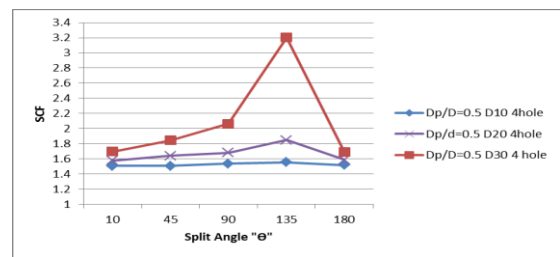


Fig.4.3: Variation of SCF for  $D_p/D = 0.5$  (4-holes)

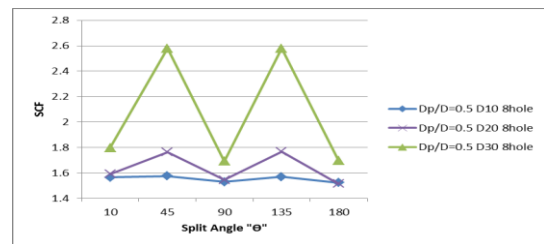


Fig. 4.4: Variation of SCF for  $D_p/D = 0.5$  (8-holes)

Fig. 4.3 indicates that the SCF in rotating split ring remain almost constant up to 90° then it suddenly increases till split angle of 135° and decreases till 180° split angle. It observed that the maximum SCF is for the split angle of 135°.

In fig. 4.4, it is observed that the hole diameter of 30 mm leads to maximum SCF in the split ring. It is seen that the hole diameter of 10 mm SCF leads to increase in the SCF with respect to split angle variation.

Variation of SCF for  $D_p/D=0.6$  are shown in fig. 4.5 and 4.6

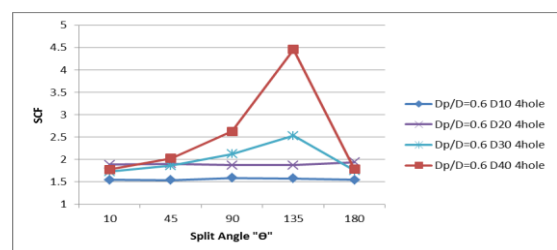


Fig. 4.5: Variation of SCF for  $D_p/D = 0.6$  (4-holes)

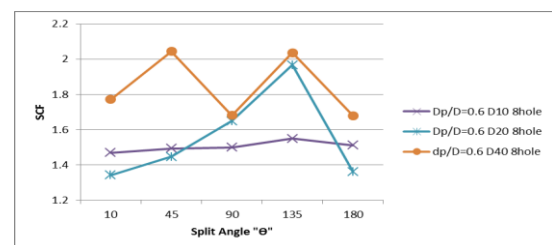


Fig. 4.6: Variation of SCF for  $D_p/D = 0.6$  (8-holes)

Fig. 4.5 indicates that the stress concentration factor in rotating split ring, remain almost constant up to 135° and decreases till 180° split angle. It observed that the maximum

SCF is for the split angle of  $135^{\circ}$ . It is seen that the hole diameter of 10 mm SCF leads to increase in the SCF with respect to split angle variation.

In Fig. 4.6, it is observed that the hole diameter of 40 mm induces maximum SCF. It is observed that the maximum SCF is for the split angle of  $45^{\circ}$  and  $135^{\circ}$ . It is seen that the hole diameter of 10 mm SCF leads to constant increase in the SCF with respect to split angle variation.

Variation of SCF for  $D_p/D=0.7$  are shown in fig. 4.7 and 4.8

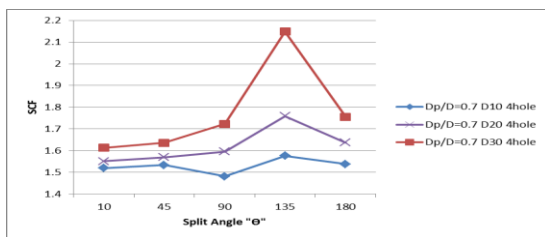


Fig. 4.7: Variation of SCF for  $D_p/D = 0.7$  (4-holes)

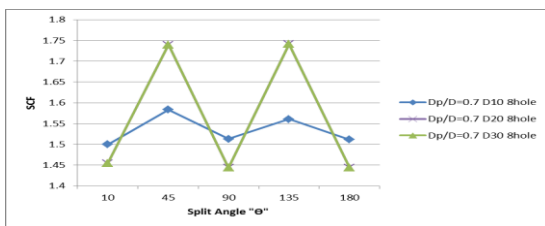


Fig. 4.8: Variation of SCF for  $D_p/D = 0.7$  (8-holes)

Fig. 4.7 indicates that the SCF in rotating split ring remain almost constant up to  $135^{\circ}$  and decreases till  $180^{\circ}$ . It is observed that the maximum SCF is for the split angle of  $135^{\circ}$ .

In fig. 4.8, it is observed that hole diameter of 20 mm and 30 mm are having approximately same magnitude of SCF. It is seen that the hole diameter of 10 mm, leads to increase in the SCF with respect to split angle variation.

Variation of SCF for  $D_p/D=0.8$  are shown in fig. 4.9 and 4.10

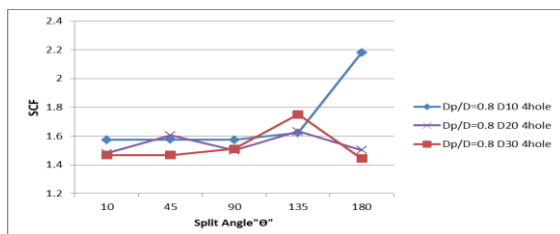


Fig. 4.9: Variation of SCF for  $D_p/D = 0.8$  (4-holes)

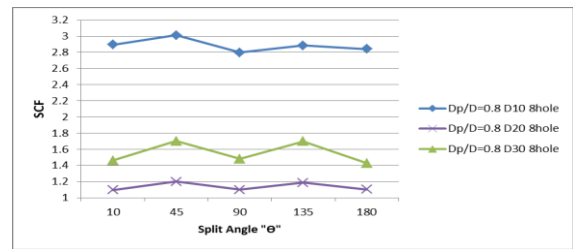


Fig. 4.10: Variation of SCF for  $D_p/D = 0.8$  (8-holes)

Fig. 4.9 indicates that the SCF in rotating split ring remain almost constant up to  $135^{\circ}$  and decreases till  $180^{\circ}$ . It is observed that the maximum value of SCF is for the split angle of  $180^{\circ}$ .

In fig. 4.10, it is observed that, the diameter of hole of 10 mm is having maximum values of SCF as compare to other hole diameters.

Variation of SCF for  $D_p/D=0.9$  are shown in fig. 4.11 and 4.12

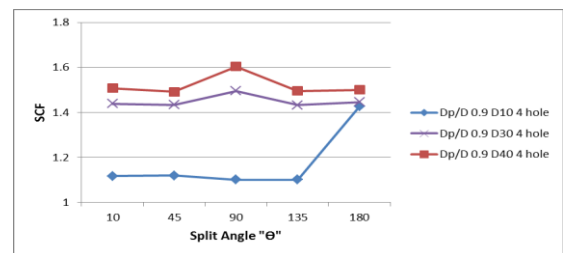


Fig. 4.11: Variation of SCF for  $D_p/D = 0.9$  (4-holes)

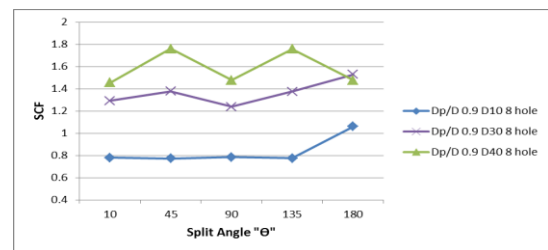


Fig. 4.12: Variation of SCF for  $D_p/D = 0.9$  (8-holes)

Fig. 4.11 indicates that the SCF in rotating split ring remain almost constant up to  $90^{\circ}$  and decreases till  $180^{\circ}$  but it differ for diameter of hole 10mm. It is observed that the maximum value of SCF is for the split angle of  $90^{\circ}$ .

Fig. 4.12 it is seen that the hole diameter of SCF leads to constant increase up to  $180^{\circ}$ . It is observed that the maximum value of SCF is for the split angle  $45^{\circ}$  &  $135^{\circ}$ .

Variation of SCF for  $D_p/D=1.0$  are shown in fig. 4.13 and 4.14

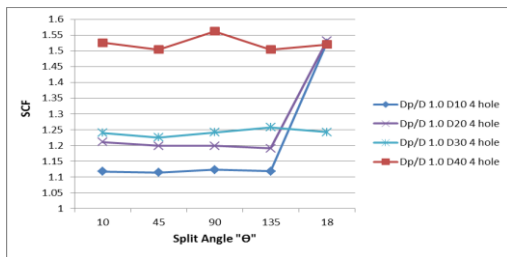


Fig. 4.13: Variation of SCF for Dp/D = 1.0 (4-holes)

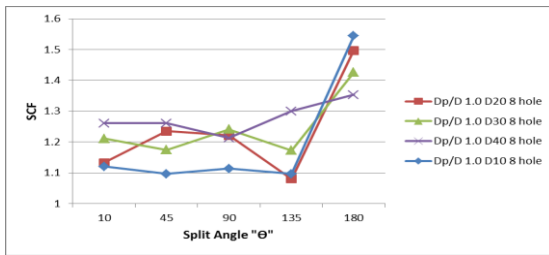


Fig. 4.14: Variation of SCF for Dp/D = 1.0 (8-holes)

Fig. 4.13 indicates that the SCF in rotating split ring remain almost constant up to 135° then it suddenly increases till split angle of 180°. It observed that the maximum SCF value is for the split angle of 90°.

Fig. 4.14 indicates that the SCF in rotating split ring remain almost constant variation up to 135° then it suddenly increases till split angle of 135°. It observed that the maximum value of SCF is for the split angle of 180°.

### 5. STRESS ANALYSIS OF SOLID SPLIT RING SUBJECTED TO BENDING LOAD

The finite element approach is used to evaluate the stresses in the rotating split ring with central hole by varying the split angles as 10°, 45°, 90°, 135° and 180°. The bending load is applied by considering the pressure of P = 100 N/mm<sup>2</sup> acting normal to the split faces. The figures 5.1 shows the geometry of solid split ring and 5.2 shows the Von-mises stress contour for various split angles. The FE results are given in Table 5.1.

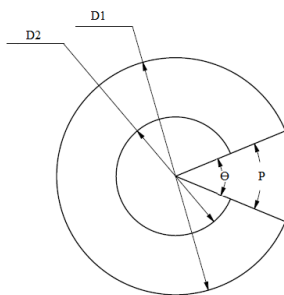


Fig. 5.1: Geometry of split ring subjected to bending load

Table 5.1: Stress Analysis of Solid Split Ring

Solid Split Ring			
Split angle "θ"	1st Principle stress N/mm <sup>2</sup>	2 <sup>nd</sup> Principle stress N/mm <sup>2</sup>	Von-mises stress (σ) N/mm <sup>2</sup>
10°	101.3	32.48	99.96
45°	108.4	35.09	116.3
90°	112.4	32.84	112.5
135°	101.7	32.94	109.3
180°	92.21	29.53	93.63

The variation of Von-mises stresses with respect to split angle are shown in fig. 5.3.

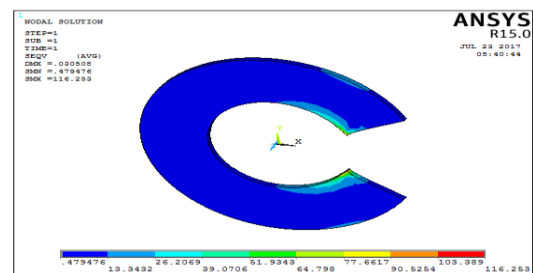


Fig. 5.2: Von-mises stress contour for solid split ring

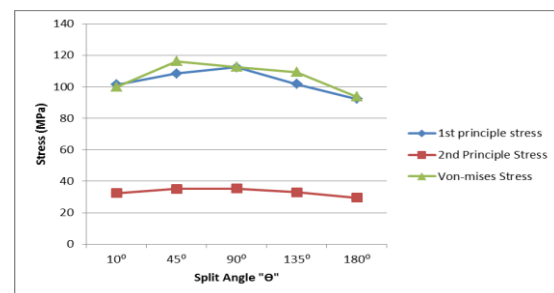


Fig. 5.3: Variation of Stresses with Respect to Split Angle

As per fig. 5.3, the behavior of 1st Principle stress and Von-mises stress with respect to split angle is similar having maximum stress value for split angle of 45° and later on it reduces till split angle of 180°. The 2<sup>nd</sup> principle stress shows marginal variation of stress magnitude with respect to split angle.

### 6. STRESS ANALYSIS OF SPLIT RING WITH HOLES SUBJECTED TO BENDING LOAD

The finite element approach is used to evaluate the stress of split ring subjected to bending moment (Load P = 100 N/mm<sup>3</sup>) by changing the split angles as 10°, 45°, 90°, 135° and 180°. In this study, the following cases are considered to evaluate the stress in split ring subjected to bending moment with 4-hole and 8-hole which are situated at pitch circle diameter corresponding to the various ratio of D<sub>p</sub>/D.



- Case 1: Split ring with holes, for  $D_p/D = 0.5$
- Case 2: Split ring with holes, for  $D_p/D = 0.6$
- Case 3: Split ring with holes, for  $D_p/D = 0.7$
- Case 4: Split ring with holes, for  $D_p/D = 0.8$
- Case 5: Split ring with holes, for  $D_p/D = 0.9$
- Case 6: Split ring with holes, for  $D_p/D = 1.0$

Figure 6.1 & 6.2 shows the representative Von-mises stress contour for 4 number of hole and 8 number of hole for  $D_p/D=0.5$ .

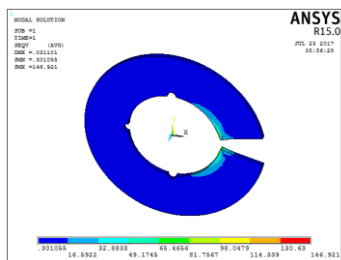


Fig. 6.1: Von-Mises Stress Contour for 4 Holes

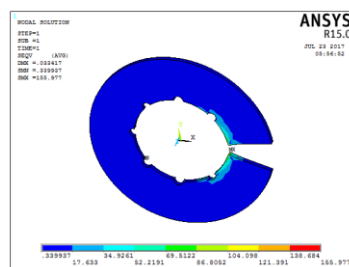


Fig. 6.2: Von-Mises Stress Contour for 8 Holes

The variation of Von-mises stress for varies cases with variation of split angle are shown in fig. 6.3 to 6.14

Variation of Von-mises stresses for  $D_p/D=0.5$  are shown in fig. 6.3 and 6.4

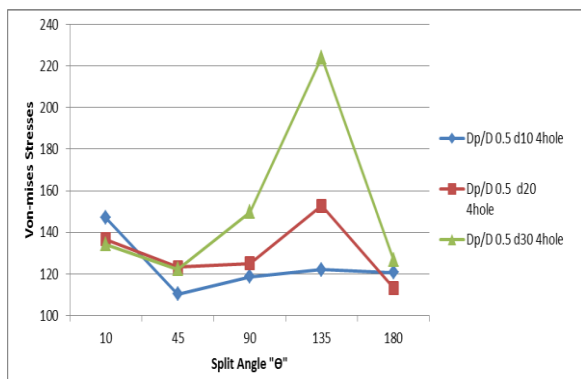


Fig.6.3: Variation of Stresses for  $D_p/D = 0.5$  (4-holes)

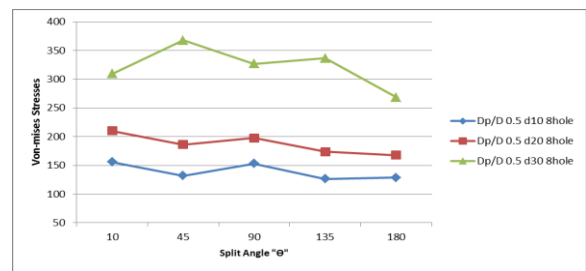


Fig. 6.4: Variation of Stresses for  $D_p/D = 0.5$  (8-holes)

Fig. 6.3 indicates that the stresses in split ring subjected to bending moment remain almost constant up to  $135^\circ$  then it decreases till  $180^\circ$ . It is observed that the maximum stress is for the split angle of  $135^\circ$ .

Fig. 6.4 indicates that the stresses in split ring decreases up to  $180^\circ$ . It observed that the maximum stress is for the split angle of  $45^\circ$ .

Variation of Von-mises stresses for  $D_p/D=0.5$  are shown in fig. 6.5 and 6.6

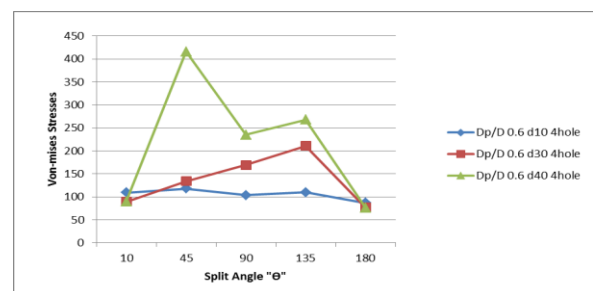


Fig 6.5: Variation of Stresses for  $D_p/D = 0.6$  (4-holes)

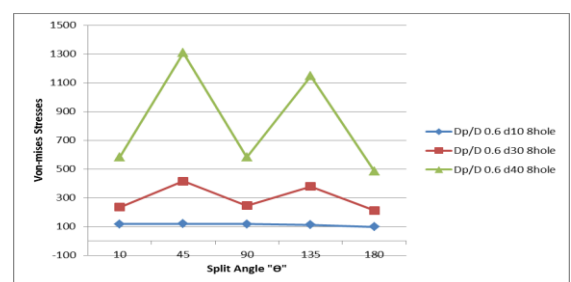


Fig. 6.6: Variation of Stresses for  $D_p/D = 0.6$  (8-holes)

In fig. 6.5, it is observed that the stresses in split ring remain constant variation up to  $135^\circ$  then it decreases till split angle of  $180^\circ$ . It observed that the maximum stress is for the split angle of  $45^\circ$ .

In fig. 6.6, it is observed that the hole diameter of 40 mm induces maximum stresses in the split ring. It is seen that the hole diameter of 10 mm leads to constant stress with respect to split angle variation.

Variation of Von-mises stresses for  $D_p/D=0.5$  are shown in fig. 6.7 and 6.8

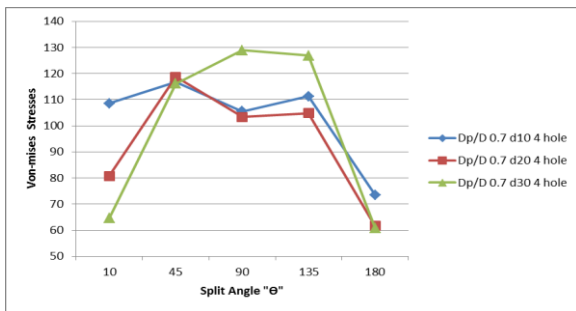


Fig. 6.7: Variation of Stresses for  $D_p/D = 0.7$  (4-holes)

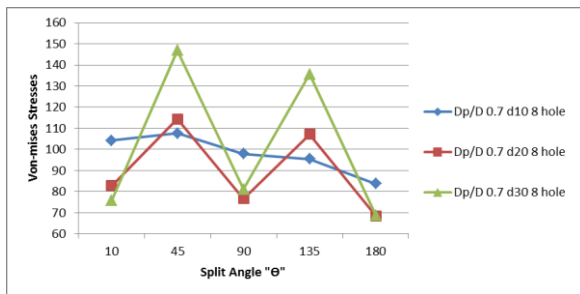


Fig. 6.8: Variation of Stresses for  $D_p/D = 0.7$  (8-holes)

Fig. 6.7 indicates that the stresses in split ring subjected to bending moment rises up to  $45^\circ$  then it decreases till  $180^\circ$  split angle. It observed that the maximum stress is for the split angle of  $90^\circ$ .

In fig. 6.8 it is observed that the hole diameter of 30 mm induces maximum stresses in the split ring. It is seen that the hole diameter of 10 mm induces stresses constant decrease with respect to split angle variation. It is observed that the hole diameter of 20 mm and 30 mm minimum magnitude stresses in split ring is approximately same.

Variation of Von-mises stresses for  $D_p/D=0.5$  are shown in fig. 6.9 and 6.10

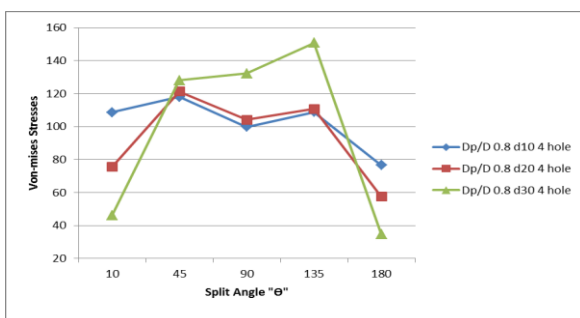


Fig. 6.9: Variation of Stresses for  $D_p/D = 0.8$  (4-holes)

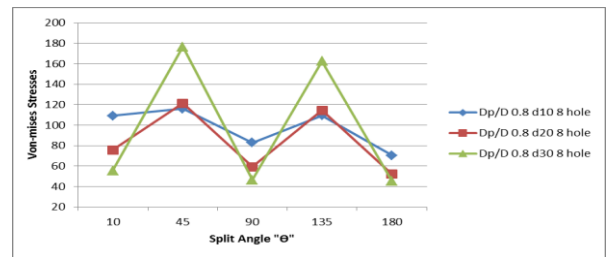


Fig. 6.10: Variation of Stresses for  $D_p/D = 0.8$  (8-holes)

Fig. 6.9 indicates that the stresses in split ring subjected to bending moment rises up to  $45^\circ$  then it decreases till  $180^\circ$  of split angle. It is observed that the maximum stress is found for the split angle of  $135^\circ$ .

In fig. 6.10 it is observed that the hole diameter 30 mm induces maximum stresses in the split ring. It is seen that the hole diameter 10 mm and 20 mm similarly having maximum marginal magnitude stresses. It is observed that the stresses decrease with increases the split angle of split ring.

Variation of Von-mises stresses for  $D_p/D=0.5$  are shown in fig. 6.11 and 6.12

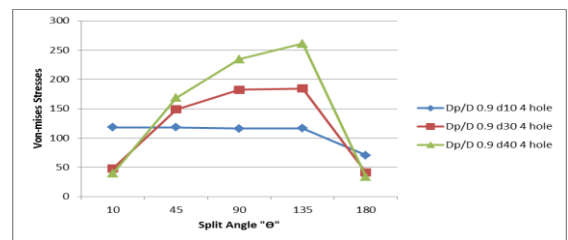


Fig. 6.11: Variation of Stresses for  $D_p/D = 0.9$  (4-holes)

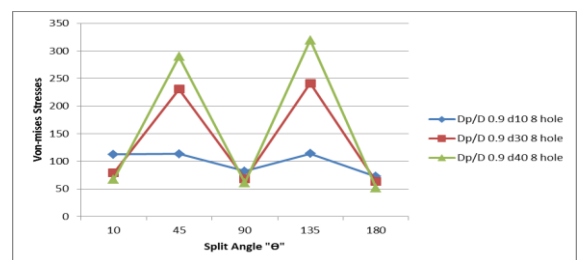


Fig. 6.12: Variation of Stresses for  $D_p/D = 0.9$  (8-holes)

Fig. 6.11 indicates that the stresses in split ring subjected to bending moment rises up to  $135^\circ$  then it decreases till  $180^\circ$  of split angle. It observed that the maximum stress is for the split angle of  $135^\circ$ .

In fig. 6.12, it is observed that the hole diameter 40 mm induces maximum stresses in the split ring. It is seen that the hole diameter 30 mm and 40 mm similarly having maximum marginal magnitude stresses. It is observed that

the hole diameter 10 mm induces small variation in stresses with respect to split angle.

Variation of Von-mises stresses for  $D_p/D=0.5$  are shown in fig. 6.13 and 6.14

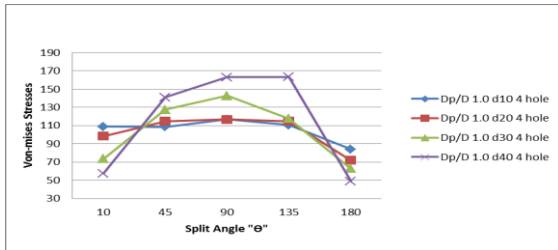


Fig.6.13: Variation of Stresses for  $D_p/D = 1.0$  (4-holes)

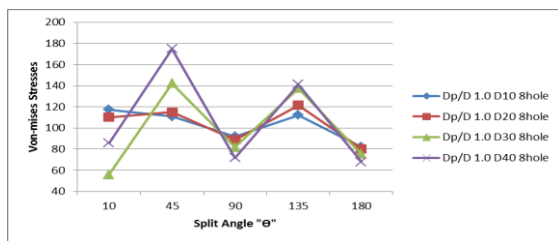


Fig.6.14: Variation of Stresses for  $D_p/D = 1.0$  (8-holes)

Fig. 6.13 indicates that the stresses in split ring subjected to bending moment rises up to  $90^\circ$  then it decreases till  $180^\circ$  split angle. It observed that the maximum stress is for the split angle of  $135^\circ$ .

In fig. 6.14, it is observed that the stresses decrease with increase in the split angles. It is observed that the maximum stresses induced in the hole diameter 40 mm.

## 7. CONCLUSIONS

From the present analysis it is observed that the split angle influences the stresses in rotating ring without discontinuities with stress rise as per increase in split angle.

The analysis of the rotating split ring with discontinuities for various split angles indicates that there is abrupt rise in the stress magnitudes with size of discontinuities and split angle. This is attributed to the stress concentration effect occurring due to discontinuities.

The analysis of split ring without discontinuities subjected to bending moment revealed that the stress magnitudes varies with respect to split angle and it is observed that the Von-mises stresses decreases with increase in the split angle with some exceptions.

The analysis of the split ring with discontinuities subjected to bending moment for various split angles indicated that there is abrupt rise in the stress magnitudes with size of

discontinuities and split angle. This is attributed to the stress concentration effect occurring due to discontinuities.

These findings may serve as guidelines for designing the split ring with discontinuities subjected to rotation & bending load.

## SCOPE FOR FUTURE WORK

The future scope of work with reference to this work is as follows.

- In the present work, the analysis of the split ring is carried out by Finite Element Method (FEM). The similar analysis can be carried out using experimental method of strain gauges and result can be verified.
- The analysis of split ring with and without discontinuities can be carried out using photo-elastic analysis.
- The effect of non-circular discontinuities on the stresses in the split ring can also be studied.

## REFERENCES

- [1] D. Kornack and P. Rakic, "Cell Proliferation without Neurogenesis in Adult Primate Neocortex," Science, vol. 294, Dec. 2001, pp. 2127-2130, doi:10.1126/science.1065467.
- [2] E. Dragoni, A. Strozzi. "Analysis of a split ring inserted into a circular housing" journals of strain analysis, vol. 21, no 2, 1986, pp. 59.
- [3] Bandeta, c., Nicolich m and Strozzi, a. "On the Bursting Mechanism in Rotating Ring", journals of strain analysis, vol. 28[3], 1993, pp.153-162.
- [4] M. Batista F. Kosel "Stress Concentration of Open Complete Rotating Ring" journals of strain analysis, vol. 30, 1995.
- [5] J.N. Sharma, Dinkar Sharma, Sheo Kumar "Stress and strain analysis of rotating FGM thermo-elastic circular disk by using FEM" International Journal of Pure and Applied Mathematics Vol. 74, 2012, pp.339-352.
- [6] J. N. Sharma, "Analysis of Stresses and Strains in a Rotating Homogeneous Thermo-elastic Circular Disk by Using Finite Element Method", International Journal of Computer Applications (0975 - 8887) Vol. 35, December 2011, pp. 13.
- [7] Niraj Pandey "FEA of Piston Ring by Using ABAQUS" International Journal of Scientific & Engineering Research, Volume 6, 1864 ISSN 2229-5518, Issue 4, April-2015.



- [8] Babak Haghpanah, Jahromi Hamid, Nayeb-Hashemi, Ashkan Vaziri, "Elasto-Plastic Stresses in a Functionally Graded Rotating Disk", Department of Mechanical and Industrial Engineering, Northeastern University, Boston, MA 02115.
- [9] Lateef. I.A., Kareem. E. A. Jan., "Simulation Effects of Increasing the Piston Ring Radial Thickness on the Piston Ring Gap", International Journal of Engineering and Applied Sciences, Vol. 6, year. 2015, ISSN2305-8269, pp. 01.
- [10] Alma žiga, aleksandar karač, dušan vukojević publish on Analitička i numerička analiza naprežanja u nosivom prstenu rotacijske peći "Analytical and numerical stress analysis of the rotary kiln ring" ISSN 1330-3651 (Print), ISSN 1848-6339 (Online) UDC/UDK 621.783.23-477:539.377.384.388]: pp. 519.